

ORIGINAL ARTICLE

Natural volcanic CO₂ seeps reveal future trajectories for host–microbial associations in corals and sponges

Kathleen M Morrow, David G Bourne, Craig Humphrey, Emmanuelle S Botté, Patrick Laffy, Jesse Zaneveld, Sven Uthicke, Katharina E Fabricius and Nicole S Webster
Australian Institute of Marine Science, P.M.B. 3, Townsville, Queensland, Australia

Atmospheric carbon dioxide (CO₂) levels are rapidly rising causing an increase in the partial pressure of CO₂ (pCO₂) in the ocean and a reduction in pH known as ocean acidification (OA). Natural volcanic seeps in Papua New Guinea expel 99% pure CO₂ and thereby offer a unique opportunity to explore the effects of OA *in situ*. The corals *Acropora millepora* and *Porites cylindrica* were less abundant and hosted significantly different microbial communities at the CO₂ seep than at nearby control sites <500 m away. A primary driver of microbial differences in *A. millepora* was a 50% reduction of symbiotic *Endozoicomonas*. This loss of symbiotic taxa from corals at the CO₂ seep highlights a potential hurdle for corals to overcome if they are to adapt to and survive OA. In contrast, the two sponges *Coelocarteria singaporensis* and *Cinachyra* sp. were ~40-fold more abundant at the seep and hosted a significantly higher relative abundance of *Synechococcus* than sponges at control sites. The increase in photosynthetic microbes at the seep potentially provides these species with a nutritional benefit and enhanced scope for growth under future climate scenarios (thus, flexibility in symbiosis may lead to a larger niche breadth). The microbial community in the apparently pCO₂-sensitive sponge species *S. massa* was not significantly different between sites. These data show that responses to elevated pCO₂ are species-specific and that the stability and flexibility of microbial partnerships may have an important role in shaping and contributing to the fitness and success of some hosts.

The ISME Journal (2015) 9, 894–908; doi:10.1038/ismej.2014.188; published online 17 October 2014

Introduction

Declining seawater pH, termed ocean acidification (OA), is a direct result of increasing atmospheric carbon dioxide (CO₂) that leads to higher partial pressure of CO₂ (pCO₂) in seawater. Rising pCO₂ reduces the concentration of carbonate ions and the saturation state of calcium carbonate minerals, which are essential for calcification in carbonate-accreting invertebrates such as corals. Volcanic CO₂ seeps provide a unique opportunity to investigate how organisms respond to OA *in situ* (Hall-Spencer *et al.*, 2008; Fabricius *et al.*, 2011). Within the D'Entrecasteaux Island group in Milne Bay Province, Papua New Guinea, tropical coral reef communities exist within natural volcanic seeps that continuously expel ~99% pure CO₂ into the sediments and water column (Fabricius *et al.*, 2011). The water chemistry, temperature, currents and light

of the seep environment is otherwise consistent with reef sites <500 m away, providing a unique opportunity to study organisms in an un-manipulated natural pCO₂/pH experiment. The composition of reef organisms along the pCO₂/pH gradient between seep and non-seep sites varies such that as pH declines, so does the richness of structurally complex corals (e.g., branching, foliose and tabulate growth forms), crustose coralline algae, foraminifera, soft corals and a range of other macro-invertebrates (Fabricius *et al.*, 2011; Uthicke *et al.*, 2013; Fabricius *et al.*, 2014). Although many of the same species are found inside and outside of the CO₂ seeps, the most abundant benthic organisms living at reduced pH are massive *Porites* spp., non-calcareous macroalgae and seagrass. Sponge communities are also common at these shallow water CO₂ seeps with recent surveys revealing that some species can tolerate extreme pH conditions, whereas others are particularly vulnerable to elevated CO₂ (Goodwin *et al.*, 2013). However, at the community level, there appears to be a significant decline in sponge cover from normal to high CO₂ sites (Fabricius *et al.*, 2011; Goodwin *et al.*, 2013).

Corals and sponges rely on intimate and dynamic associations with diverse microorganisms for their

Correspondence: NS Webster, A healthy and Resilient GBR, Australian Institute of Marine Science, PMB 3 Townsville Mail Centre, Townsville, Queensland 4810, Australia.
E-mail: n.webster@aims.gov.au

Received 22 May 2014; revised 18 August 2014; accepted 21 August 2014; published online 17 October 2014

health and physiology, yet little is known about how their microbiota respond to changes in $p\text{CO}_2$. The ability of microbes to rapidly evolve means they can shift their host range, metabolic capabilities and other essential functions in response to changing environmental conditions. Thus, to predict the response and resilience of marine organisms under future climate scenarios, we need to understand how their associated microbiota responds to increasing $p\text{CO}_2$. An increase in CO_2 or reduction in pH can have consequences for microbially driven nutrient cycling, including carbon and nitrogen fixation (Hutchins *et al.*, 2007), nitrification (Beman *et al.*, 2011) and iron availability (Shi *et al.*, 2010). CO_2 enrichment studies in microcosms have documented distinct and seasonal changes in pelagic microbial communities (Krause *et al.*, 2012), with some bacteria demonstrating enhanced growth efficiency and increased CO_2 fixation at elevated $p\text{CO}_2$ (Teira *et al.*, 2012). Bacteria may even profit energetically if the homeostatic difference between external and internal pH (7.4 to 7.8) is reduced (Padan *et al.*, 2005). Most previous studies were conducted on pelagic bacteria and it is unknown whether such microbial shifts and physiological changes also occur within host-associated communities. Furthermore, whether such changes compromise host health or infer an adaptive advantage has not yet been explored. Aquarium-based studies have shown that increased $p\text{CO}_2$ or reduced pH can cause microbial shifts in communities associated with corals, foraminifera and crustose coralline algae (Meron *et al.*, 2011; Webster *et al.*, 2013a,b). However, to date, no study has explored microbial communities in organisms that have spent their entire lives at elevated CO_2 , with the potential for their communities to adapt or physiologically acclimatize over large timescales (>3 years).

Coral-associated microbial communities are composed of a core population of species-specific bacteria, in addition to transient associates that can vary in response to geographic location, climate and other environmental factors (Ritchie, 2006). Some coral species support highly specific associations, such as the coral *Porites astreoides* in the Caribbean and *Stylophora pistillata* in the Red Sea, which both host microbiomes largely composed of bacteria in the family *Hahellaceae* (*Endozoicomonas* sp.; (Morrow *et al.*, 2012; Bayer *et al.*, 2013a,b), whereas other corals have more diverse associations (Bourne *et al.*, 2013). The significance of these diversity differences has not yet been fully elucidated although it is believed that this has an important role in host fitness and stability in changing environmental conditions. Marine sponges are also known to host dense, diverse and highly stable microbial communities with many of the microorganisms being specific to sponge hosts (Simister *et al.*, 2012). Environmental disturbances such as temperature, bleaching, disease, nutrient enrichment and changes in pH can all

cause dramatic changes in both coral and sponge microbiota (Webster *et al.*, 2008; Vega Thurber *et al.*, 2009; Meron *et al.*, 2011; Fan *et al.*, 2012; Vega Thurber *et al.*, 2014). Symbiotically conferred stress tolerance has been demonstrated in a number of systems (Rodriguez *et al.*, 2008) and may provide a strategy for withstanding the effects of climate change and/or OA. The current study uses 16S rRNA gene amplicon pyrosequencing to assess the $p\text{CO}_2$ /pH sensitivity of microbial associations within two coral and three sponge species and explore whether host tolerance to OA stress could be enabled *via* habitat-adapted microbial associations.

Materials and methods

Sample collection and processing

Sponge and coral abundance was surveyed at the volcanic shallow water CO_2 seep system (Upa Upasina) within the D'Entrecasteaux Islands, Milne Bay Province, Papua New Guinea (PNG; 9°49.45' S, 150°49.07' E), and at a nearby ambient $p\text{CO}_2$ 'control' site not exposed to elevated $p\text{CO}_2$ (<500 m from the seeps, 9°49.68' S, 150°49.23' E; (Fabricius *et al.*, 2011; Uthicke *et al.*, 2013). Sponge abundance was surveyed across five transects (20 m × 1 m) within each site in 2011 (depth 3–4 m). Coral abundance was surveyed across 15 transects (10 m × 0.5 m) at each site in 2014 to determine the abundance of *Acropora* spp. and other CO_2 -sensitive coral species, including *P. cylindrica*.

Replicate samples of *Acropora millepora* ($n=10$) and *Porites cylindrica* ($n=5$) coral colonies and *Coelocarteria singaporensis*, *Cinachyra* sp. and *Stylissa massa* sponge individuals ($n=8-10$ per species per site) were collected on SCUBA from both the high $p\text{CO}_2$ seep site and the ambient control site. Seawater carbonate chemistry varies in response to bubble activity and water motion at the seep; thus, corals experience a pH range of 7.91–8.09 (Avg. $p\text{CO}_2$ 346 μatm) at the control site and pH 7.28–8.01 (Avg. $p\text{CO}_2$ 624 μatm) at the seep site (Fabricius *et al.*, 2014), which is within the range of future predictions for the year 2100 (Moss *et al.*, 2010). Coral and sponge tissue samples were transported to the surface in individual plastic bags and immediately preserved in 95% ethanol within 15 ml falcon tubes and stored at -20°C for transport back to the Australian Institute of Marine Science (AIMS).

Tissues from sampled coral colonies were removed with sterile tips and pressurized air into the original preservation ethanol, then transferred to Beckman Ultra-clear centrifuge tubes (Beckman-Coulter, Brea, CA, USA), and pelleted in a swinging bucket rotor (20 000 g for 15 min at 4°C). Each pellet was resuspended using PowerPlant Pro Microbead solution (MoBio Laboratories, Carlsbad, CA, USA), transferred to MoBio microbead tubes and frozen at -20°C . Samples were later thawed at 65°C for 10 min and extracted using the PowerPlant Pro DNA

Isolation Kit as per the manufacturer's instructions (MoBio Laboratories). DNA was also extracted from all sponge samples using MoBio PowerPlant DNA Isolation Kit as per the manufacturer's instructions.

16S gene-targeted pyrosequencing

Extracted DNA was quantified using a NanoDrop 2000 UV-vis spectrophotometer (Wilmington, DE, USA), and aliquoted to the same concentration (20 ng µl⁻¹). All samples were PCR amplified with universal bacterial primers targeting the hypervariable region V1-V3 of the 16S ribosomal rRNA gene with 28F (5'GAGTTTGATCNTGGCTCAG3') and 519R (5'GTNTTACNGCGGCKGCTG3') and sequenced at the Molecular Research Laboratories (Shallowater, TX, USA). Briefly, a single-step 30-cycle PCR using the HotStarTaq Plus Master Mix Kit (Qiagen, Valencia, CA, USA) was used under the following conditions: 94 °C for 3 min, followed by 28 cycles of 94 °C for 30 s; 53 °C for 40 s and 72 °C for 1 min; after which a final elongation step at 72 °C for 5 min was performed. Following PCR, all amplicon products were mixed in equal concentrations and purified using Agencourt AMPure beads (Beckman Coulter), followed by sequencing using the Roche (Basel, Switzerland) 454 FLX+ platform and Titanium reagents.

Sequencing and statistical analyses

Raw.sff sequence reads from all samples were denoised and processed through the MOTHUR software package (www.mothur.org) and the analysis protocol was based on the 454 standard operating procedure (Schloss *et al.*, 2011). Briefly, sequences of length <200 bp, ambiguous base calls or homopolymer runs exceeding 8 bp were removed. Sequences were aligned with the SILVA 16 S rRNA alignment (Pruesse *et al.*, 2007) as a reference and operational taxonomic units (OTUs) were defined using Pre.cluster after removal of singleton sequences, clustering at 3% divergence (97% similarity). Chimeric artefacts were also removed using UCHIME (Edgar *et al.*, 2011). OTUs were taxonomically classified using a BLAST-based method against the May 2013 curated Greengenes database ((Altschul *et al.*, 1997; DeSantis *et al.*, 2006), <http://greengenes.secondgenome.com/>), and compiled at each taxonomic level into a counts file. Any sequences that were classified as Mitochondria, Eukaryotic or Chloroplast as well as any sequences of unknown origin were filtered out of the dataset. Sequences without hits were rechecked against the NCBI-nr database (<http://www.ncbi.nlm.nih.gov/>) for 16S rRNA gene sequences retrieved from uncultured bacteria using a BLAST search (Altschul *et al.*, 1997) with the E-value threshold (0.001). Data from each coral and sponge species were analysed separately and each rarefied to account for variation in sampling depth. The raw pyrosequencing reads were submitted to the NCBI

Sequence Read Archive under accession numbers PRJNA253930 for corals and SRP029239 for sponges.

Alpha diversity statistics including total observed and predicted Chao1 (Chao, 1984) OTUs and the Shannon *H'* diversity statistic were calculated in MOTHUR and plotted. OTU tables were built in Microsoft Excel from two MOTHUR output files (SHARED and TAXONOMY), and pivot tables were used to condense tables by phyla and family for graphical interpretation. OTU data were square-root-transformed and similarity percentage (SIMPER) analyses were performed to examine which OTUs contributed most to the dissimilarity between sites. Bray-Curtis distance matrices were built to examine additional patterns of community structure and visualized using principal coordinate analyses. Pearson correlation vectors were overlaid to demonstrate which taxa have strong positive or negative correlations with either PCO axis, indicative of site differences. A permutational analysis of variance (PERMANOVA, using 10 000 permutations) determined whether spatial separation between sites was statistically significant. All multidimensional statistical analyses were performed in PRIMER V6 with the PERMANOVA+ add-on (PRIMER-E Ltd., Devon, UK).

Functional profile prediction for key symbionts

To better understand the potential functional contributions of the observed shifts in microbial diversity, we imputed functional profiles for two key microbial symbionts in the PICRUSt software package ((Langille *et al.*, 2013), <http://picrust.github.io/picrust/>). This technique estimates the genomic copy number of each gene family (KO) in an environmental microorganism based on the position of that organism in a reference phylogeny with regard to microorganisms for which finished genomes are available. Hidden state prediction (Zaneveld and Vega Thurber, 2014) is then used to model changes in each gene family over time, and estimate mean and 95% confidence intervals for the abundance of each gene family.

Functional profile imputation was performed on partial 16S rRNA gene sequences for the *Endozoicomonas* (Gammaproteobacteria: Oceanospirillales) symbiont of *A. millepora* (Otu_0002; 256 bp) and the *Synechococcus* (Cyanobacteria: Synechococophycideae) symbiont of *C. singaporensis* (Otu_0001; 125 bp). These sequences were mapped to the Greengenes 13_8 reference phylogeny (McDonald *et al.*, 2012) using `pick_closed_reference_otus.py` script of the QIIME 1.8 software package (Caporaso *et al.*, 2010), running in the MacQIIME environment. Functional profiles, Nearest Sequenced Taxon Index (NSTI) scores and 95% confidence intervals were calculated using the PICRUSt's `predict_metagenomes.py` script, treating each OTU as a separate sample. Following functional imputation, the

obtained profiles of gene family abundance across samples were summarized into KEGG Pathways using the `categorize_by_function.py` PICRUSt script (PICRUSt counts genes that participate in multiple KEGG pathways once per pathway).

Results

Community abundance surveys

Previous coral abundance surveys conducted at the volcanic CO₂ seep in Milne Bay reported that both coral species, *A. millepora* and *P. cylindrica*, were significantly less abundant at the seep than at the adjacent control site (see Fabricius *et al.*, 2011). Surveys repeated in March 2014 confirm a significant reduction in *Acropora* spp. (~ two times less abundant) and *P. cylindrica* (~ five times less abundant) at the seep site in comparison with the control site (ANOVA, $F_{(1,33)} = 20.6$, $P < 0.001$ and $F_{(1,33)} = 11.4$, $P = 0.002$, respectively; Figure 1). Sponge surveys showed that *S. massa* was ~ six times less abundant at the seep than at the control site (ANOVA, $F_{(1,10)} = 12.0$, $P = 0.006$; Figure 1). In contrast, both *C. singaporensis* and *Cinachyra* sp.

were almost 40 times more abundant at the CO₂ seep than at the control site (ANOVA, $F_{(1,10)} = 8.6$, $P = 0.015$; $F_{(1,10)} = 17.5$, $P = 0.002$, respectively; Figure 1).

Coral-associated bacterial communities

A total of 193 724 high-quality 16S rRNA gene pyrosequencing reads were recovered for both coral species from the seep and control sites, with an average of 6457 ± 1213 reads per sample. Each coral species was analysed separately and retrieved sequences were rarefied to the sample with the least reads (1426 reads for *A. millepora* and 1850 reads for *P. cylindrica*) (Table 1). Both coral species hosted a number of unique bacterial phyla, including 27 phyla represented in *A. millepora* and 30 in *P. cylindrica*. The most abundant and diverse phylum recovered from both coral species was the *Proteobacteria* (Figure 2). *P. cylindrica* hosted higher bacterial diversity than *A. millepora*, with a significant reduction in microbial diversity at the phylum level at the high pCO₂ site ($H' = 7.2 \pm 0.34$

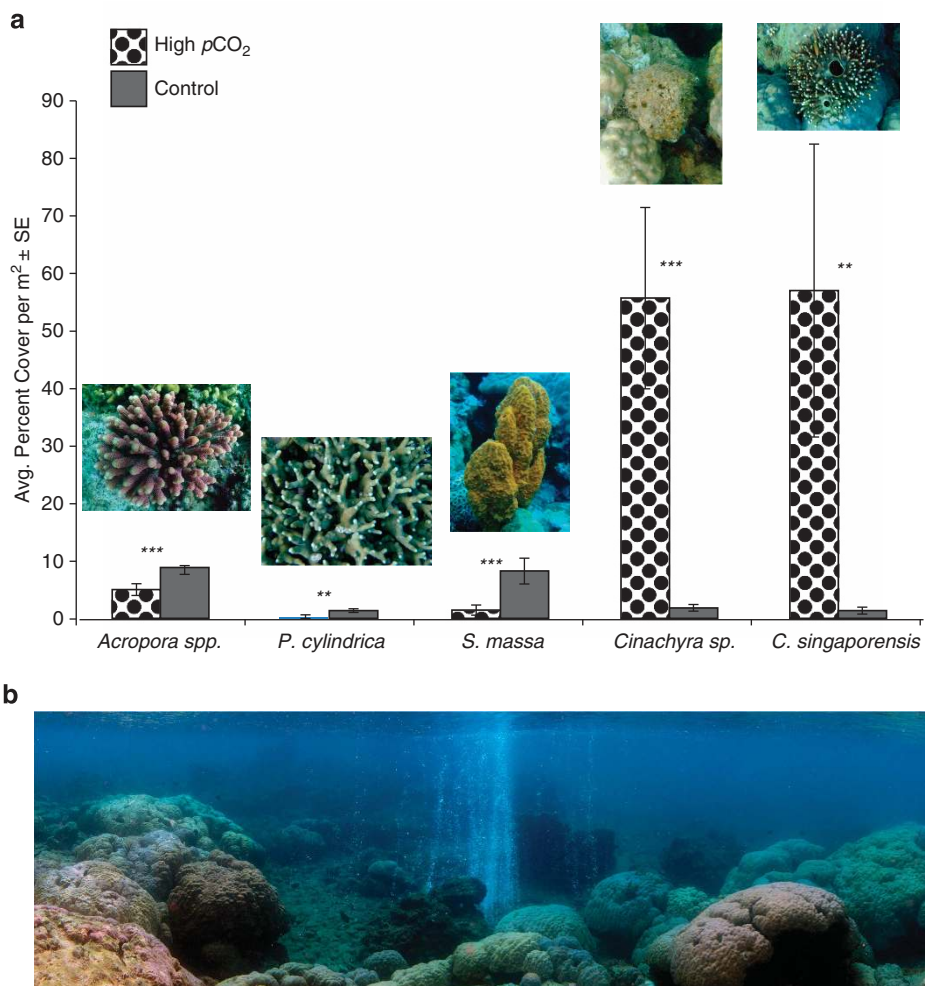


Figure 1 (a) Sponge and coral percent cover per m². (b) Panorama of the PNG seep site. Photo: S. Noonan.

Table 1 Alpha diversity statistics based on sequences derived from two coral species and three sponge species in the control and high pCO₂ seep sites

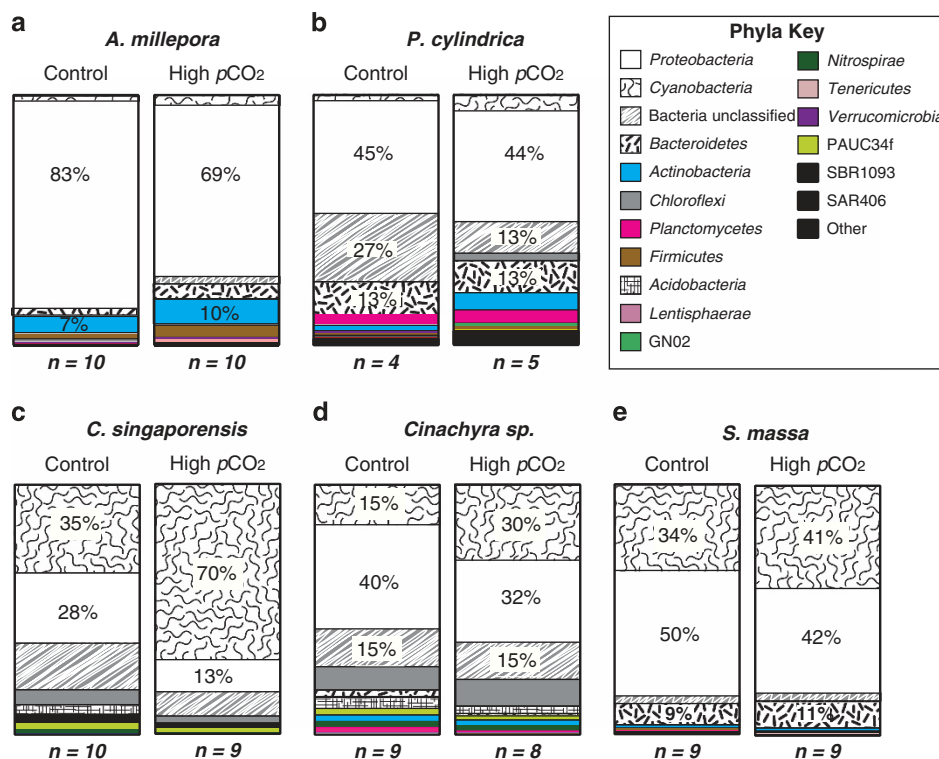
	<i>A. millepora</i>		<i>P. astreoides</i>		<i>C. coelocarcteria</i>		<i>Cinachyra sp.</i>		<i>S. massa</i>	
	Control (10) ^a	High pCO ₂ (10)	Control (4)	High pCO ₂ (5)	Control (10)	High pCO ₂ (9)	Control (9)	High pCO ₂ (8)	Control (9)	High pCO ₂ (9)
Avg # Trimmed Seqs	6488 ± 2462	3463 ± 534	10 274 ± 3954	5848 ± 1863	5520 ± 961	7393 ± 1116	9478 ± 753	5320 ± 431	5399 ± 680	6043 ± 1703
# Rarefied Seqs	1426		1850		2420		2568		2148	
Greengenes OTUs	1528		2794		3279		6348		2744	
Unique OTUs ^b	431		449		140		448		267	
Chao1	208 ± 20	216 ± 21	595 ± 70	789 ± 66	389 ± 89	558 ± 61	1322 ± 130	1394 ± 198	395 ± 26	446 ± 33
Observed	145 ± 9	141 ± 10	261 ± 40	439 ± 48	135 ± 33	209 ± 22	431 ± 44	602 ± 86	191 ± 11	202 ± 8

Abbreviations: OTUs, operational taxonomic units; pCO₂, partial pressure of CO₂.

Average alpha diversity statistics ± s.e. calculated with alpha_diversity.py in qiime_VirtualBox.

^aNumber in parentheses indicates samples included in analyses (n=#).

^bNumber of unique OTUs after all identical OTUs exported from Mothur were combined.

**Figure 2** Average percent contribution to total abundances of most dominant phyla across all species replicates. (a) *A. millepora*, (b) *P. cylindrica*, (c) *C. singaporensis*, (d) *Cinachyra sp.* and (e) *S. massa*. n = the total number of individual sponges or coral colonies sampled for each species at each site.

s.e.) compared with the control site ($H' = 5.3 \pm 0.5$ s.e.; $F_{(1,7)} = 10.7$, $P = 0.01$; Figure 3).

At the bacterial species level (97% sequence similarity), significant differences in community composition were observed between sites in both *A. millepora* (PERMANOVA Pseudo- $F_{1,19} = 1.68$, $P = 0.002$) and *P. cylindrica* (Pseudo- $F_{1,8} = 1.23$, $P = 0.007$; Figure 4). Significant differences in *A. millepora* microbes between sites were the direct result of changes in the relative abundance of OTUs affiliated with members of the *Proteobacteria* (Figure 4, Table 2). The relative abundance of most *Proteobacteria* sequences increased in corals

at the CO₂ seeps, except for sequences associated with the class *Gammaproteobacteria*. In particular, sequences associated with the genus *Endozoicomonas* sp. (class *Gammaproteobacteria*, family *Hahellaceae*) were two times less abundant in *A. millepora* at the seep compared with the control site (26.4 vs 51.6%; Table 2). SIMPER analysis and Pearson correlation vectors associated with principal coordinate analyses plots also indicate that members of the *Endozoicomonas* sp. were particularly affected by the differences in environmental and host-related conditions between seep and control sites (Figure 4, Table 3). Most other *Gammaproteobacteria* affiliated

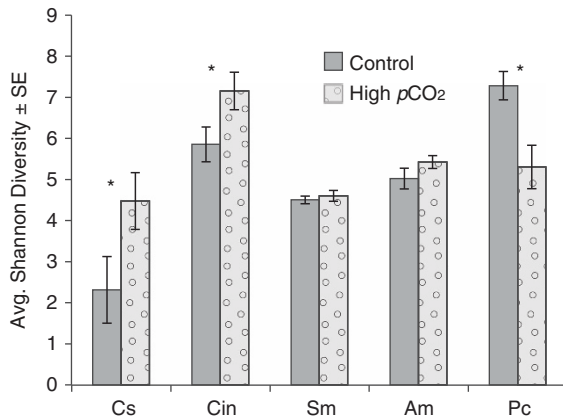


Figure 3 Shannon Diversity index: means \pm s.e. The asterisk indicates significant difference at $\alpha < 0.05$.

sequences from *A. millepora* also decreased at the seep site in comparison with the control, except for sequences within the family *Halomonadaceae*, which increased in relative abundance from 1.2 to 4.8% of the total microbiome at high pCO₂ (Table 2). In contrast, the relative abundance of sequences associated with many other coral-associated bacterial phyla increased at the CO₂ seep in comparison with the adjacent control site (e.g., *Actinobacteria*, *Bacteroidetes*, *Cyanobacteria*, *Firmicutes*; Table 2).

Porites cylindrica also demonstrated a decrease in OTUs affiliated with the *Gammaproteobacteria* at the seep compared with the control site (Table 2), especially in the three families *Alteromonadaceae* (11.4–1.1% of the total microbiome), *Pseudoalteromonadaceae* (8.1–0.7%), and *Vibrionaceae* (2.0–0.8%, Table 2). The only group that increased at the seep site were purple sulphur bacteria in the family *Chromatiaceae* (0.2–4.2% of the total microbiome), mostly composed of bacteria associated with the genus *Rheinheimera* sp. (Table 2). SIMPER analyses indicate that members of the *Alteromonadaceae* and *Pseudoalteromonadaceae* influence site differences in the community structure for *P. cylindrica* (Table 3). Members of the phylum *Bacteroidetes* composed approximately 13% of the *P. cylindrica* microbiome at both sites, but they varied in composition (Table 2). For example, bacteria in the class *Flavobacteria* increased in relative abundance (1.3–7.0% of the total microbiome), and *Cytophaga* decreased in relative abundance (6.0–3.0%) at the seep site in comparison with the control (Table 2). Furthermore, members of the *Bacteroidetes* phylum are indicated by Pearson correlation vectors and SIMPER analyses as influencing site differences (Table 3, Figure 4). The relative abundance of several other bacterial phyla (e.g., *Actinobacteria*, *Cyanobacteria*, *Planctomycetes* and *Chloroflexi*) increased in abundance at the CO₂ seep in comparison with the control site (Table 2). Interestingly, both corals demonstrate a twofold increase in

Cyanobacteria-affiliated OTUs from approximately 2.5% of the total microbiome at the control site to 6% at the seep site (Table 2).

Sponge-associated bacterial communities

A total of 373 494 high-quality 16S rRNA reads were recovered from all three sponge species with an average of 6163 ± 279 s.e. reads per sample (Table 1). Samples from each sponge species were rarefied to the lowest retrieved number of sequences, ranging from 2148 to 2568 reads (Table 1). Each sponge species hosted a number of unique bacterial phyla including 15 hosted by *C. singaporensis*, 30 hosted by *Cinachyra* sp. and 18 hosted by *S. massa*. Like in corals, *Proteobacteria* were the most abundant and diverse phylum in *Cinachyra* sp and *S. massa*, although *C. singaporensis* was dominated by *Cyanobacteria*, particularly at the seep site (70%, Figure 2). Among the three sponge species, *Cinachyra* sp. hosted the highest bacterial diversity at the high pCO₂ site ($H' = 7.2 \pm 0.5$) in comparison with the control (Shannon $H' = 5.9 \pm 0.4$; ANOVA $F_{(1,15)} = 4.3$ $P = 0.05$; Figure 3).

At the bacterial species level (97% sequence similarity), significant differences in community composition between sites were detected for the two pCO₂-tolerant sponge species *C. singaporensis* (PERMANOVA $F = 3.18$, $P = 0.03$) and *Cinachyra* sp. ($F = 2.07$, $P = 0.001$; Figure 4). The only species examined that did not differ in microbial community composition between the seep and control site was the apparently pCO₂-sensitive sponge species *S. massa* ($F = 1.12$, $P > 0.05$; Figure 4). OTUs affiliated with *Synechococcus* sp. and *Proteobacteria* were responsible for much of the between-site differences in both *C. singaporensis* and *Cinachyra* sp. (Figure 4) and these *Synechococcus* sp. OTUs were clearly distinct from the cyanobacterial OTUs observed within the two corals (Table 3). A twofold increase in *Cyanobacteria* (*Synechococcus* spp.) from the control to the seep site was observed in both *C. singaporensis* (35–70% of the total microbiome) and *Cinachyra* sp. (1–30%), whereas *Cyanobacteria* showed only a marginal increase in *S. massa* (34–41%; Figure 2, Table 2). SIMPER analyses also demonstrated that *Synechococcus* sp. was the major driver of differences between seep and non-seep bacterial communities for *C. singaporensis* and *Cinachyra* sp. (Table 3). In addition to *Synechococcus* spp., a large number of less-discriminating bacterial OTUs also contributed to the between-site variation (Figure 4). The increase in *Cyanobacteria* corresponded to a relative decrease in classes *Alpha*-, *Beta*-, *Delta*- and *Gammaproteobacteria* in all sponges at the seep site in comparison with the control (Table 2). In addition, concomitant with the elevated abundance of *Cyanobacteria* in *C. singaporensis* and *Cinachyra* sp. at the seep was a generally lower relative abundance of phyla containing known

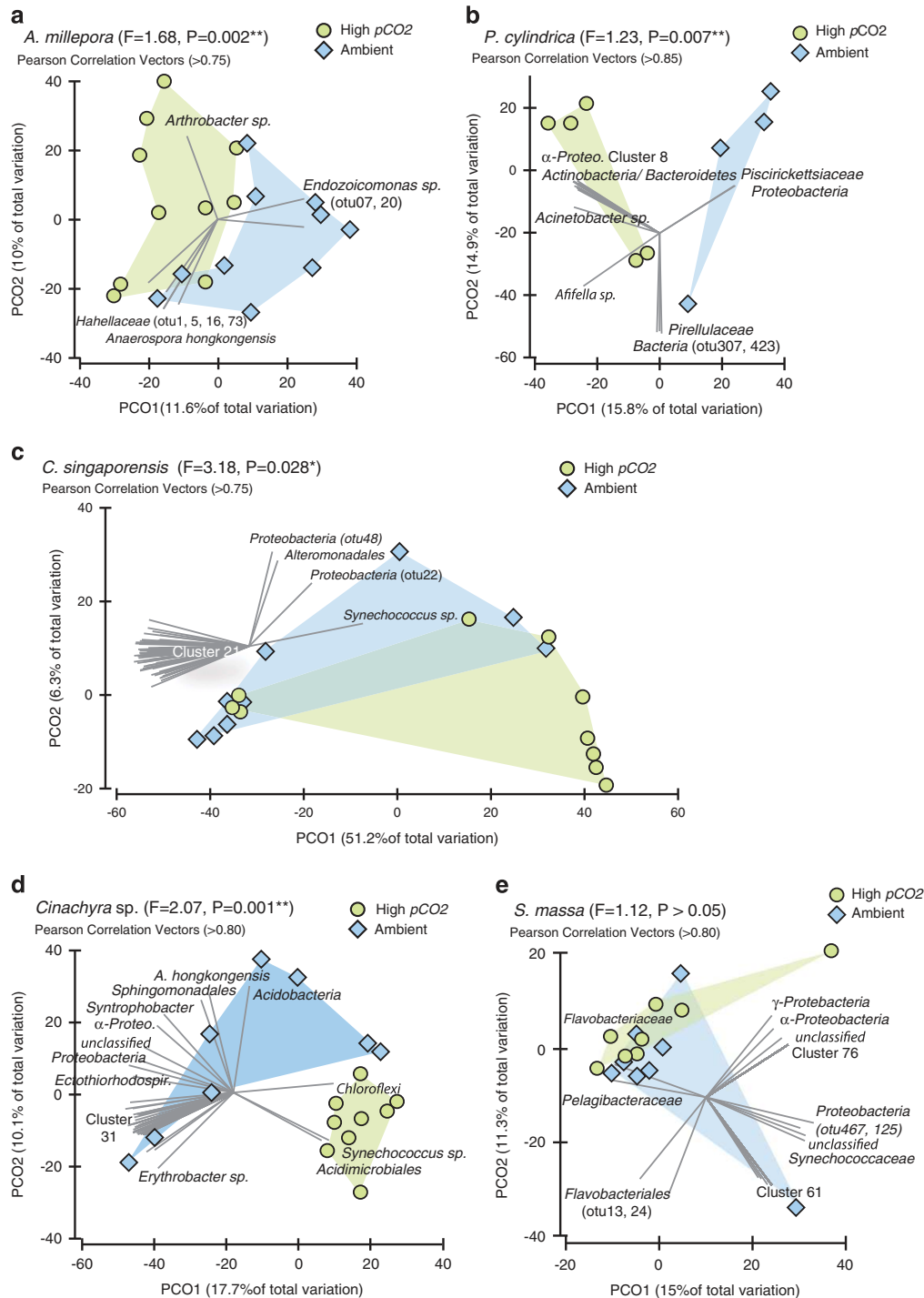


Figure 4 Principal coordinate analysis plots for each coral and sponge species based on square-root transformed Bray-Curtis distances. (a) *A. millepora*, (b) *P. cylindrica*, (c) *C. singaporensis*, (d) *Cinachya* sp. and (e) *S. massa*. Green circles indicate bacterial communities sampled at the seep sites (high $p\text{CO}_2$ and low pH), and blue diamonds represent samples from adjacent control locations. Pearson correlation vectors represent the most resolved taxonomy for bacterial OTUs. PERMANOVA. Pseudo-F and P -values are reported. The list of taxa composing the OTU clusters is available in Supplementary Material.

sponge symbionts. For example, in *C. singaporensis*, *Chloroflexi* declined from 3.8 to 5.8 to 2.7%, *Acidobacteria* declined from 3.8 to 5.1%, *Deltaproteobacteria* declined from 3.6 to 1.3% and *Nitrospirae* declined from 1.3 to 0.4%. (Figure 2, Table 2). Similarly, in *Cinachya* sp., *Acidobacteria* declined from 4.6 to 2.9%, *Planctomycetes* declined from 1.9 to

0.6% and *Bacteroidetes* declined from 2.6 to 1.1% (Figure 2, Table 2). In contrast, with the exception of *Cyanobacteria* and *Bacteroidetes*, which both showed a marginal but non-significant increase at the seep, the distribution of OTUs within phyla in *S. massa* were consistent across both sites (Figure 2).

Table 2 Relative abundance of OTUs affiliated with dominant phyla

<i>a. A. millepora</i>	Control	High pCO ₂	<i>a. C. singaporensis</i>	Control	High pCO ₂	% of Total
Proteobacteria (% of Total)	83.5	68.8	Proteobacteria (% of Total)	23.3	10.8	0.1–0.5
<i>Alphaproteobacteria</i>	14.4	19.8	<i>Alphaproteobacteria</i>	2.8	2.3	0.6–1.0
<i>Caulobacteraceae</i>	3.5	2.6	<i>Pelagibacteraceae</i>	0.3	0.2	1.1–2.5
<i>Rhodobacteraceae</i>	2.4	2.9	unclassified	2.3	2.0	2.5–5.0
<i>Sphingomonadaceae</i>	1.5	0.8	<i>Deltaproteobacteria</i>	3.6	1.3	5.1–7.5
unclassified	3.7	6.9	<i>Syntrophobacteraceae</i>	0.9	0.4	7.6–10
<i>Betaproteobacteria</i>	2.2	4.4	<i>Entotheonellaceae</i>	2.6	0.8	10.1–25
<i>Comamonadaceae</i>	1.4	3.4	<i>Gammaproteobacteria</i>	0.6	0.3	> 25%
<i>Gammaproteobacteria</i>	66.2	43.2	HTCC2089	2.9	1.6	
<i>Hahellaceae</i>	51.6	26.4	HTCC2188	0.5	0.4	
<i>Enterobacteriaceae</i>	1.8	0.6	unclassified	11.2	5.2	
<i>Halomonadaceae</i>	1.2	4.8	Cyanobacteria (% of Total)	35.0	70.1	
<i>Moraxellaceae</i>	3.7	2.9	<i>Synechococcaceae</i>	35.0	70.0	
<i>Pseudoalteromonadaceae</i>	1.5	0.5	unclassified	0.1	0.1	
<i>Pseudomonadaceae</i>	2.7	3.1				
<i>Actinobacteria</i>	6.55	9.82	<i>b. Cinachyra sp.</i>	Control	High pCO ₂	
<i>Bacteroidetes</i>	2.72	5.72	Proteobacteria (% of Total)	39.6	31.8	
<i>Cyanobacteria</i>	2.05	4.19	<i>Alphaproteobacteria</i>	15.9	7.2	
<i>Firmicutes</i>	1.82	4.65	<i>Rhodobacteraceae</i>	6.6	2.8	
unclassified	1.48	2.90	<i>Rhodospirillaceae</i>	0.4	0.2	
			<i>Pelagibacteraceae</i>	0.7	0.8	
<i>b. P. cylindrica</i>	Control	High pCO ₂	unclassified	6.5	3.5	
Proteobacteria (% of Total)	45.0	43.8	<i>Deltaproteobacteria</i>	0.5	0.2	
<i>Alphaproteobacteria</i>	13.1	20.7	unclassified	0.1	0.1	
<i>Rhodobacteraceae</i>	1.6	4.1	<i>Gammaproteobacteria</i>	19.2	16.3	
<i>Rhodobiaceae</i>	1.4	1.1	HTCC2089	1.3	2.6	
unclassified	7.6	11.1	<i>Piscirickettsiaceae</i>	0.9	0.2	
<i>Betaproteobacteria</i>	0.4	1.8	OM60	0.3	0.2	
<i>Deltaproteobacteria</i>	0.5	1.3	<i>Alteromonadaceae</i>	0.3	0.1	
<i>Gammaproteobacteria</i>	29.9	16.1	<i>Colwelliaceae</i>	0.1	0.1	
<i>Alteromonadaceae</i>	11.4	1.1	unclassified	15.2	12.5	
<i>Chromatiaceae</i>	0.2	4.2	Cyanobacteria (% of Total)	14.7	30.0	
<i>Pseudoalteromonadaceae</i>	8.1	0.7	<i>Synechococcophycideae</i>	9.9	25.8	
<i>Vibrionaceae</i>	2.0	0.8	<i>Synechococcaceae</i>	7.2	25.7	
unclassified	1.5	8.9	<i>Pseudanabaenaceae</i>	2.6	0.1	
Bacteroidetes (% of Total)	13.3	12.8	<i>Oscillatoriohycideae</i>	0.6	0.4	
<i>Bacteroidia</i>	0.3	0.4	<i>Cyanobacteriaceae</i>	0.0	0.2	
<i>Cytophagia</i>	6.0	3.0	<i>Phormidiaceae</i>	0.0	0.1	
<i>Flavobacteriia</i>	1.3	7.0	unclassified	0.3	0.1	
<i>Saprospirae</i>	1.9	0.2				
unclassified	3.0	2.0	<i>c. S. massa</i>	Control	High pCO ₂	
<i>Actinobacteria</i>	2.22	7.18	Proteobacteria (% of Total)	46.7	38.8	
<i>Cyanobacteria</i>	2.47	6.64	<i>Alphaproteobacteria</i>	16.0	15.3	
<i>Planctomycetes</i>	3.70	5.39	<i>Pelagibacteraceae</i>	12.7	10.6	
<i>Chloroflexi</i>	0.76	3.02	<i>Rhodobacteraceae</i>	2.6	4.2	
unclassified	3.00	2.00	AEGEAN_112	0.3	0.2	
			unclassified	0.1	0.1	
			<i>Deltaproteobacteria</i>	6.3	2.0	
			unclassified	6.2	1.9	
			<i>Gammaproteobacteria</i>	23.1	20.7	
			<i>Halomonadaceae</i>	1.8	3.6	
			unclassified	20.5	16.5	
			Cyanobacteria (% of Total)	33.9	40.5	
			<i>Synechococcophycideae</i>	31.4	38.0	
			<i>Synechococcaceae</i>	31.4	37.9	
			Bacteroidetes (% of Total)	8.2	10.0	
			<i>Cytophagia</i>	1.6	2.3	
			<i>Flammeovirgaceae</i>	1.6	2.3	
			<i>Flavobacteriia</i>	2.9	3.5	

Abbreviation: OTUs, operational taxonomic units.

Functional implications of community shifts

To summarize some of the potential functional contributions of key symbionts, functional profiles were predicted for the major *Endozoicomonas* symbiont lost in *A. millepora* near the seep site and *Synechococcus* that increased in *C.*

singaporensis using the PICRUSt software package. This approach uses evolutionary modelling to put bounds on the gene content of environmental organisms based on their sequenced relatives. The accuracy of the method is highest when closely related reference genomes are available. The validity

Table 3 Similarity Percentage Analysis (SIMPER) for 10 most significant OTUs driving differences between the CO₂ seep and control site

Phylum	Most resolved taxonomy (Blastn)	"Otu"	Higher abundance		Fold difference	Rank
			High pCO ₂	Ambient		
<i>A. millepora</i> dissimilarity = 85.17%						
Actinobacteria	<i>Corynebacterium vitaeruminis</i>	Otu0008		x	1.02	9
Proteobacteria						
Alphaproteobacteria	<i>Brevundimonas</i> sp.	Otu0010		x	2.46	10
Gammaproteobacteria						
Hahellaceae	unclassified	Otu0001		x	0.53	1
Hahellaceae	unclassified	Otu0005		x	0.24	7
Hahellaceae	<i>Endozoicomonas</i> sp.	Otu0002		x	6.65	2
Hahellaceae	<i>Endozoicomonas</i> sp.	Otu0003		x	4.39	3
Hahellaceae	<i>Endozoicomonas</i> sp.	Otu0007		x	5.12	4
Hahellaceae	<i>Endozoicomonas numazuensis</i>	Otu0006		x	3.89	5
Halomonadaceae	<i>Chromohalobacter salexigens</i>	Otu0013	x		3.88	8
Bacteria	unclassified	Otu0004	x		0.99	6
<i>P. cylindrica</i> dissimilarity = 94.8%						
Actinobacteria	<i>Corynebacterium vitaeruminis</i>	Otu0007	x		1.6	6
Bacteroidetes	Flavobacteriaceae	Otu0006	x		3.83	7
Cyanobacteria	Oscillatoriothycideae	Otu0001		x	3.66	1
Proteobacteria						
Alphaproteobacteria	unclassified	Otu0018	x		3.97	9
Gammaproteobacteria						
Alteromonadaceae	<i>Candidatus Endobugula</i>	Otu0004		x	5.23	4
Chromatiaceae	<i>Rheinheimera</i> sp.NG3	Otu0013	x		4.04	10
Pseudoalteromonadaceae	<i>Pseudoalteromonas</i> sp. RKVR13	Otu0005		x	5.22	3
Pseudoalteromonadaceae	<i>Pseudoalteromonas</i> sp.EF1A-B164	Otu0009		x	4.47	5
Bacteria	unclassified	Otu0003		x	5.37	2
Bacteria	unclassified	Otu0002		x	4.48	8
<i>C. singaporensis</i> avg. dissimilarity = 71.85%						
Cyanobacteria	<i>Synechococcus</i> sp.	Otu0001	x		13.68	1
Proteobacteria						
Deltaproteobacteria	Entotheonellaceae	Otu0008		x	3.63	6
Gammaproteobacteria	unclassified	Otu0004		x	4.54	2
	unclassified	Otu0005		x	3.74	5
	unclassified	Otu0010		x	3.41	8
Bacteria	unclassified	Otu0002		x	5.69	3
	SBR1093	Otu0003		x	4.64	4
	unclassified	Otu0006		x	3.27	7
	PAUC34f	Otu0007		x	2.57	9
	unclassified	Otu0009		x	2.96	10
<i>Cinachyra</i> sp. avg. dissimilarity = 79.42%						
Actinobacteria	Acidimicrobiales	Otu00030	x		3.76	10
Cyanobacteria	<i>Synechococcus</i>	Otu00001	x		16.13	1
	<i>Synechococcus</i>	Otu00002	x		2.07	6
Proteobacteria	unclassified	Otu00005	x		8.45	2
Gammaproteobacteria	unclassified	Otu00010	x		7.07	3
	unclassified	Otu00003		x	2.64	4
	HTCC2089	Otu00006	x		3.19	8
Nitrospirae	Nitrospiraceae	Otu00007	x		1.1	5
Bacteria	unclassified	Otu00016	x		3.91	7
Bacteria	PAUC34f	Otu00012		x	2.67	9
<i>S. massa</i> avg. dissimilarity = 47.06%						
Alphaproteobacteria	Pelagibacteraceae	Otu0006		x	2.01	5
	Pelagibacteraceae	Otu0004		x	0.75	10
Cyanobacteria	<i>Synechococcus</i> sp.	Otu0001	x		2.57	3
	Synechococcaceae	Otu0012		x	0.64	6
	Synechococcaceae	Otu0030	x		0.45	9

Table 3 (Continued)

Phylum	Most resolved taxonomy (Blastn)	"Otu"	Higher abundance		Fold difference	Rank
			High pCO ₂	Ambient		
<i>Proteobacteria</i>						
<i>Deltaproteobacteria</i>	unclassified	Otu0005		x	4.59	2
<i>Gammaproteobacteria</i>	<i>Candidatus Portiera</i>	Otu0017	x		1.44	8
	<i>Thiohalorhabdales</i>	Otu0003	x		0.97	4
	unclassified	Otu0002		x	4.40	1
	unclassified	Otu0009	x		1.05	7

Abbreviation: OTUs, operational taxonomic units.

of reference genomes can be quantified using the NSTI score, which is simply the average branch length on the reference phylogeny between the organism(s) to be predicted and an organism for which a genome sequence is available (Langille *et al.*, 2013). Sufficiently close reference genomes were available for the *C. singaporensis* *Synechococcus* symbiont (NSTI 0.056), whereas available genomic data were at the outer limits of accurate prediction for the *Endozoicomonas* symbiont of *A. millepora* (NSTI 0.156). On the basis of previous cross-validation studies of all sequenced genomes, these NSTI scores suggest that a balanced accuracy of ~0.95 should be expected for prediction of gene family presence/absence (for genes in KEGG KOs) in the *Synechococcus* and ~0.85 for the *Endozoicomonas* (Langille *et al.*, 2013, Supplementary Figure 1). Dominant KEGG Pathways for *Synechococcus* included photosynthesis, membrane transport, and DNA repair and recombination (Supplementary Figure 1). Dominant KEGG Pathways in the *Endozoicomonas* from *A. millepora* included pathways for membrane transporters, ABC transporters, two-component signalling systems, cell motility and secretion (Supplementary Figure 1).

These imputed functional profiles largely reflected the known roles of these organisms. The *Synechococcus* functional profile included many genes involved in photosynthesis pathways, whereas these were absent or at very low abundance in the heterotrophic *Endozoicomonas*. Conversely, *Endozoicomonas* were marked by high abundances of membrane transporters (~1.7 × their abundance in *Synechococcus*), motility genes and two-component signalling systems. Both profiles included poorly characterized gene families within their top three KEGG Pathways. Although not atypical in bacteria, the abundance of gene families with poorly characterized function in both abundant symbionts highlights the potential for unexplored functional novelty in these groups.

Discussion

Compared with preindustrial levels, global oceans have already experienced a 30% increase in acidity,

and are predicted to undergo a further 170% increase in acidity by 2100 (IGBP, IOC, SCOR, 2014), leading to reduced biogenic calcification (Anthony *et al.*, 2008), increased bio-erosion (Fang *et al.*, 2013) and significant changes to coral reef community structure (Hall-Spencer *et al.*, 2008; Fabricius *et al.*, 2011, 2014). This study assessed how the microbiomes of key reef invertebrates might respond to OA *in situ*, by surveying corals and sponges that have had a post-larval lifetime of exposure to elevated CO₂ within a volcanic CO₂ seep. The composition of invertebrate-associated microbial communities is known to be intimately linked to host health (Bourne and Webster, 2013), and we therefore predicted that OA-sensitive species would host microbial communities that are clearly distinct from the same species under ambient conditions, including a potential loss of putative symbionts and the appearance of microorganisms from taxa commonly associated with stress and disease. Additionally, not all tropical reef organisms are detrimentally impacted by elevated pCO₂ (Fabricius *et al.*, 2011); therefore, we also hypothesized that tolerance to OA stress in some species may be enabled *via* habitat-acclimated microbial associations. Here we have shown that distinct microbial communities have developed in two sponge species that appeared to benefit from high pCO₂ / low pH conditions as well as one sponge species and two coral species that were apparently sensitive to this environment. The primary driver of microbial variation in the two sponge species that were more abundant at the seeps was an increased relative abundance of photosynthetic *Synechococcus*, whereas the major driver of variation in the apparently sensitive coral species was a loss of *Gammaproteobacteria* at the seep site, in particular the putatively endosymbiotic *Endozoicomonas* in *A. millepora*. The development of distinct microbial communities between sites may influence the fitness and success of the host, although the functional implications of these divergent microbial populations are still to be fully elucidated.

Our understanding of how OA will directly affect marine microbial communities is limited (Joint *et al.*, 2011), although microbial shifts in response to elevated pCO₂ have previously been reported

from CO₂ mesocosm experiments on bacterioplankton and picoplankton (Allgaier *et al.*, 2008; Meakin and Wyman, 2011), studies of surface-associated biofilms (Witt *et al.*, 2011) and experimental analyses of host-associated microbes (Meron *et al.*, 2011; Webster *et al.*, 2013a, 2013b; Kerfahi *et al.*, 2014). Manipulative experiments with corals exposed to high pCO₂ / low pH have demonstrated an increase in the relative abundance of disease-associated bacteria within the class *Flavobacteria* in the coral *Porites compressa* (Vega Thurber *et al.*, 2009). This is largely consistent with findings from the CO₂ seep where we also observed an increase in bacterial OTUs affiliated with *Bacteroidetes* (*A. millepora* microbiome), specifically within the class *Flavobacteria* (*P. cylindrica* microbiome). However, when two Mediterranean coral species were transplanted for 7 months into a CO₂ seep in the Gulf of Naples, Italy, and assessed by 16S rRNA gene clone sequencing, there was no detectable impact on the composition of their associated microbial communities in comparison with control sites (Meron *et al.*, 2012). Microbial community shifts reported in these previous experimental studies tend to be host- and study-specific with no microbial taxa consistently reported as present or absent from specific pH/pCO₂ treatments. It is likely that experiments conducted over extended time periods are required, particularly to enable host-associated microbial communities to adapt and reflect consistent patterns associated with environmental change. In most cases, these studies indicate that marine microbial communities can shift in response to high pCO₂, yet the speed and stability of these changes, as well as the implications for host health, adaptation, acclimation or ecosystem function, have not yet been determined.

Both coral species were less abundant and hosted significantly different microbial communities at the site of active CO₂ discharge compared with the adjacent control site. Within the *A. millepora* microbiome, a notable ~50% reduction in the family *Hahellaceae* (order *Oceanospirillales*) was observed, largely as a result of loss of sequences related to *Endozoicomonas* sp. The *Endozoicomonas* are commonly found in close association with marine invertebrates, including the deep-sea bone-eating polychaete *Osedax frankpressi* (Goffredi *et al.*, 2005), the Pacific sea slug *Elysia ornata* (Kurahashi and Yokoto, 2007), the hydrothermal vent snail *Alviniconcha* (Beinart *et al.*, 2014), in addition to gorgonians (La Rivière *et al.*, 2013; Bayer *et al.*, 2013b) and sponges (Bourne *et al.*, 2013). Associated with corals specifically, members of the genus *Endozoicomonas* have been isolated from *Montipora aequituberculata* in the Pacific (Yang *et al.*, 2010), comprise up to 80% of the microbiome of *Porites astreoides* from the Caribbean (Morrow *et al.*, 2012; Rodriguez-Lanetty *et al.*, 2013) and 70 to 95% of the microbiome in Red Sea corals *Stylophora pistillata*, *Pocillopora damicornis* and *Acropora*

humilis (Bayer *et al.*, 2013a). Importantly, a meta-analysis also revealed that *Oceanospirillales*-related sequences (which include the *Endozoicomonas* genus) were among the most common ribotypes found in healthy corals (Mouchka *et al.*, 2010), suggesting that the loss of this important taxon at high pCO₂ would have significant implications for coral health, and may contribute to the inability of these species to thrive at the CO₂ seep.

Hypotheses about the function of the *Endozoicomonas*-related symbionts have ranged from parasite consumers of host tissue to beneficial mutualists that assist in the metabolism, nutrient acquisition and/or cycling of organic compounds. The *Endozoicomonas* are members of the order *Oceanospirillales*, a group widely known to be heterotrophic and capable of degrading complex organic compounds (Garrity *et al.*, 2005), including the production of extracellular hydrolytic enzymes that can degrade various complex organic substrates such as whale bones (Goffredi *et al.*, 2007). Previous studies have also found that *Endozoicomonas* aggregate and may live endosymbiotically, including within the coral endoderm (Bayer *et al.*, 2013b), and within membrane-bound vesicles inside the gill cells of the hydrothermal vent snail *Alviniconcha* (Beinart *et al.*, 2014).

Isolates of *Endozoicomonas*-related sequences from *A. millepora* coral tissues possessed the ability to metabolise the organosulphur compound dimethylsulphoniopropionate, which suggests a role in sulphur cycling (Raina *et al.*, 2009). Furthermore, *Endozoicomonas* isolates from sponges were shown to produce the quorum-sensing metabolites N-acyl homoserine lactones (Mohamed *et al.*, 2008), and demonstrate antimicrobial activity against *Bacillus subtilis* (Rua *et al.*, 2014). In the present study, the *Endozoicomonas*-related OTUs associated with *A. millepora* that were significantly reduced at the seep site were ~96% similar to *Endozoicomonas numazuensis* (NCBI strain HC50), a strain isolated from marine sponges in Japan (Nishijima *et al.*, 2013) and similar to *E. montiporae* (Pike *et al.*, 2013), a strain isolated from the coral *Montipora aquetuberculata* (Yang *et al.*, 2010). The *E. numazuensis* strain is facultatively anaerobic and capable of fermenting carbohydrates, reducing nitrate and hydrolysing DNA (Nishijima *et al.*, 2013). Consistent with the proposed roles in nutrient acquisition and cycling of organic compounds, KEGG pathway prediction for the *A. millepora* *Endozoicomonas* OTU using PICRUSt revealed the categories of membrane transport, amino acid and carbohydrate metabolism, replication and repair, and cell motility to be the most abundant known pathways (genes of unknown function were also abundant). Taken together, these several lines of evidence suggest that host-associated *Endozoicomonas* may have important ecological roles in host health by providing otherwise unavailable macromolecular nutrients, contributing to nitrogen and/or sulphur cycling,

and shaping the associated microbial community *via* signalling molecules and antimicrobial activity.

In contrast to the observed decrease in *Endozoicomonas* at the seep site, another related bacterial genus within the family *Halomonadaceae* increased in abundance within *A. millepora*. The *Halomonadaceae* are considered coral ‘residents’ (Ritchie, 2006), are known for their successful growth over a wide range of temperature and pH levels and may produce enzymes capable of catabolizing dimethylsulphoniopropionate and acrylate produced by *Symbiodinium* within the coral tissues (Todd *et al.*, 2012). In the present study, the OTU responsible for this shift in community structure was ~99% similar to *Chromohalobacter salexigens* based on 16S rRNA gene identity (NCBI strain DSM3043), a strain isolated from high saline environments and capable of H₂S production, nitrate reduction and anaerobic growth in the presence of nitrate. Thus, although the seep environment may be suboptimal for *Endozoicomonas* sp., it may still be suitable for other putatively symbiotic members of the coral microbial community. These results suggest that coral-associated microbial communities are dynamic and responsive to changes in pCO₂ and/or pH. Although the microbial shifts reported here are not entirely consistent with previous mesocosm and laboratory studies, they do reflect host–microbial relationships that have stabilized given a lifetime of acclimation to an environment with high pCO₂.

Sponge species that are abundant at shallow water CO₂ seeps in Papua New Guinea host significantly different microbial communities to individuals of the same species at control sites less than 500 m away. Although many bacteria contribute to these differences, the variation is largely influenced by the dominance of *Synechococcus* (phylum *Cyanobacteria*) within *C. singaporensis* and *Cinachyra* sp. at the CO₂ seep. Although carbon metabolism in sponges is typically based on filter feeding of bacterioplankton, some species can obtain >50% of their carbon demand from cyanobacterial photosymbionts (Wilkinson, 1983; Cheshire and Wilkinson, 1991; Freeman and Thacker, 2011). Hosting a higher abundance of cyanobacteria may therefore lead to higher carbon fixation, but nutritional benefits may also extend to nitrogen fixation as the products of nitrogen metabolism can be transferred from the symbionts to the sponge host in some species (Freeman and Thacker, 2011). An elevated abundance of cyanobacteria likely provides at least some sponge species with enhanced scope for growth in these seep environments. Consistent with this role as providers of photosynthates, the three primary KEGG level 2 pathways identified from PICRUSt analysis of the *Synechococcus* OTU were energy metabolism (in this case, primarily pathways involved in photosynthesis), carbohydrate metabolism and amino acid metabolism.

Although research has not yet explored how symbiotic cyanobacteria respond to elevated pCO₂, recent studies of planktonic cyanobacteria have

revealed species-specific responses to CO₂ conditions projected for the end of this century (Hutchins *et al.*, 2009). For instance, at elevated pCO₂, increased rates of N₂ and CO₂ fixation occur in *Trichodesmium* (Hutchins *et al.*, 2007; Lomas *et al.*, 2012), whereas carbon assimilation in *Prochlorococcus* and *Synechococcus* is relatively unaffected by increased pCO₂ except at elevated temperatures (Fu *et al.*, 2007; Lomas *et al.*, 2012). Although pelagic *Synechococcus* spp. show an immediate increase in carbon fixation (productivity) at elevated pCO₂, this effect appears short term with acclimation of cellular physiology occurring within 1–3 days (Lomas *et al.*, 2012). However, it is important to consider that, individual strains of *Cyanobacteria* may respond differently to altered CO₂ concentrations, and these short-term experiments are unable to account for how microbes adapt and evolve in response to higher pCO₂ environments. Potential variation in photosynthetic performance of different cyanobacterial types is particularly relevant to this study where *Cyanobacteria* increased in all three sponge species and both coral species at the seep, yet only two of these sponge species were more abundant at the seep site.

In addition to improved host fitness and enhanced competitive advantage, microbial symbionts have been shown to infer environmental stress tolerance to their plant and animal hosts. For example, in the aphid *Buchnera aphidicola* symbiosis, a single nucleotide mutation of the symbiont governs the thermal tolerance of the host (Dunbar *et al.*, 2007), and in grass species from coastal and geothermal habitats, fungal endophytes confer salt and heat tolerance, respectively (Rodriguez *et al.*, 2008). On the basis of these findings, it is plausible to consider whether specific members of the microbial community in *C. singaporensis* and *Cinachyra* sp. confer low pH/high pCO₂ tolerance to the populations that occupy the CO₂ seep habitat. For instance, the internal pH of the sponge tissue may be dramatically influenced by utilisation or production of CO₂ by symbionts (e.g., *Cyanobacteria*) as well as other microbial processes such as nitrification. Transplantation experiments (potentially coupled with experimental addition of cultured symbionts) or targeted experimental analysis with microsensors would further elucidate whether these symbiont populations enhance or hinder the survival of organisms in such extreme pH environments. Furthermore, future studies at shallow CO₂ seep environments would benefit from a combination of isotope labelling experiments and metagenomic/metatranscriptomic sequencing to enhance our ability to tease apart the relative contribution of bacterial symbionts to the growth and nutrition of ‘sensitive’ and ‘tolerant’ CO₂ species.

Although the vulnerability of corals to OA is well established (Orr *et al.*, 2005), it has previously been proposed that sponges are one taxon that could benefit from projected climate change scenarios

(Bell *et al.*, 2013), potentially by acquiring microbially mediated competitive advantages that enable them to thrive under future conditions of OA. Here we have shown that distinct microbial communities have developed in two sponge species that were tolerant of the high $p\text{CO}_2$ conditions occurring within a natural volcanic CO₂ seep. Conversely, the third sponge species was significantly less abundant at the CO₂ seep and showed no flexibility in microbial symbiosis. Both coral species were also significantly less abundant at the CO₂ seep. The proposed coral symbiont *Endozoicomonas* sp. was significantly reduced in corals at the CO₂ seep, whereas the *Cyanobacteria* prominent in sponge microbiomes at the seep were present in only low abundance in the coral microbiomes. In addition, distinct microbial communities were observed in both coral species at the seep site including an overrepresentation of opportunistic bacteria previously linked with diseased and stressed corals (e.g., *Flavobacteria*). Although these results emphasise how some non-calcifying coral reef organisms (i.e., *C. singaporensis* and *Cinachyra* sp.) can benefit under reduced pH/elevated $p\text{CO}_2$ conditions, we also showed that these benefits do not extend to all species and symbiotic partnerships. Organisms that lack the flexibility (i.e., *S. massa*) to alter the composition of their symbiotic microbial community or have particularly sensitive symbiont populations (i.e., *A. millepora*, *P. cylindrica*) may be more vulnerable to the effects of OA.

Conflict of Interest

The authors declare no conflict of interest.

Acknowledgements

NSW was funded through an Australian Research Council Future Fellowship (FT120100480). The expedition to conduct the field work was funded by the Australian Institute of Marine Science.

References

- Allgaier M, Riebesell U, Vogt M, Thyrrhaug R, Grossart HP. (2008). Coupling of heterotrophic bacteria to phytoplankton bloom development at different $p\text{CO}_2$ levels: a mesocosm study. *Biogeosciences* **5**: 1007–1022.
- Altschul SF, Madden TL, Schäffer AA, Zhang J, Zhang Z, Miller W *et al.* (1997). Gapped BLAST and PSI-BLAST: a new generation of protein database search programs. *Nucleic Acids Res* **25**: 3389–3402.
- Anthony KRN, Kline DI, Diaz-Pulido G, Dove S, Hoegh-Guldberg O. (2008). Ocean acidification causes bleaching and productivity loss in coral reef builders. *Proc Natl Acad Sci USA* **105**: 17442–17446.
- Bayer T, Arif C, Ferrier-Pagès C, Zoccola D, Aranda M, Voolstra CR. (2013a). Bacteria of the genus *Endozoicomonas* dominate the microbiome of the Mediterranean gorgonian coral *Eunicella cavolini*. *Mar Ecol Prog Ser* **479**: 75–84.
- Bayer T, Neave MJ, Alsheikh-Hussain A, Hughen A, Aranda M, Yum LK *et al.* (2013b). The microbiome of the Red Sea coral *Stylophora pistillata* is dominated by tissue-associated *Endozoicomonas* bacteria. *Appl Environ Microb* **79**: 4759–4762.
- Beinart RA, Nyholm SV, Dubilier N, Girguis PR. (2014). Intracellular Oceanospirillales inhabit the gills of the hydrothermal vent snail *Alviniconcha* with chemosynthetic, γ -Proteobacterial symbionts. *Environ Microbiol Rep* doi: 10.1111/1758-2229.12183.
- Bell JJ, Davy SK, Jones T, Taylor MW, Webster NS. (2013). Could some coral reefs become sponge reefs as our climate changes? *Glob Change Biol* **19**: 2613–2624.
- Beman JM, Chow C-E, King AL, Feng Y, Fuhrman JA, Andersson AJ *et al.* (2011). Global declines in oceanic nitrification rates as a consequence of ocean acidification. *Proc Natl Acad Sci USA* **108**: 208–213.
- Bourne DG, Dennis PG, Uthicke S, Soo RM, Tyson GW, Webster NS. (2013). Coral reef invertebrate microbiomes correlate with the presence of photosymbionts. *ISME J* **7**: 1459–1459.
- Bourne DG, Webster NS. (2013). Coral Reef Bacterial Communities. In: Rosenberg E, DeLong EF, Lory S, Stackebrandt E, Thompson F (eds) *The Prokaryotes*. Springer: Berlin Heidelberg, pp 163–187.
- Caporaso JG, Kuczynski J, Stombaugh J, Bittinger K, Bushman FD, Costello EK *et al.* (2010). QIIME allows analysis of high-throughput community sequencing data. *Nat Methods* **7**: 335–336.
- Chao A. (1984). Non-parametric estimation of the number of classes in a population. *Scand J Stat* **11**: 265–270.
- Cheshire AC, Wilkinson CR. (1991). Modelling the photosynthetic production by sponges on Davies Reef, Great Barrier Reef. *Mar Biol* **109**: 13–18.
- DeSantis TZ, Hugenholtz P, Larsen N, Rojas M, Brodie EL, Keller K *et al.* (2006). Greengenes, a chimera-checked 16S rRNA gene database and workbench compatible with ARB. *Appl Environ Microb* **72**: 5069–5072.
- Dunbar HE, Wilson ACC, Ferguson NR, Moran NA. (2007). Aphid thermal tolerance is governed by a point mutation in bacterial symbionts. *PLoS Biol* **5**: e96.
- Edgar RC, Haas BJ, Clemente JC, Quince C, Knight R. (2011). UCHIME improves sensitivity and speed of chimera detection. *Bioinformatics* **27**: 2194.
- Fabricius KE, De'ath G, Noonan S, Uthicke S. (2014). Ecological effects of ocean acidification and habitat complexity on reef-associated macroinvertebrate communities. *Proc. Biol Sci* **281**: 20132479.
- Fabricius KE, Langdon C, Uthicke S, Humphrey C, Noonan S, De'ath G *et al.* (2011). Losers and winners in coral reefs acclimatized to elevated carbon dioxide concentrations. *Nat Climate Change* **1**: 165–169.
- Fan L, Liu M, Simister R, Webster NS, Thomas T. (2012). Marine microbial symbiosis heats up: The phylogenetic and functional response of a sponge holobiont to thermal stress. *ISME J* **7**: 991–1002.
- Fang JKH, Mello-Athayde MA, Schönberg CHL, Kline DI, Hoegh-Guldberg O, Dove S. (2013). Sponge biomass and bioerosion rates increase under ocean warming and acidification. *Glob Change Biol* **19**: 3581–3591.
- Freeman CJ, Thacker RW. (2011). Complex interactions between marine sponges and their symbiotic microbial communities. *Limnol Oceanogr* **56**: 1577–1586.
- Fu F-X, Warner ME, Zhang Y, Feng Y, Hutchins DA. (2007). Effects of increased temperature and CO₂ on

- photosynthesis, growth and elemental ratios of marine *Synechococcus* and *Prochlorococcus* (cyanobacteria). *J Phycol* **43**: 485–496.
- Garrity GM, Bell JA, Lilburn T. (2005). Oceanospirillales ord. nov. In Brenner DJ, Krieg NR, Garrity GM, Boone DR, De Vos P *et al.* (eds) *Bergey's Manual[®] of Systematic Bacteriology*. Springer: New York, USA, pp 270–323.
- Goffredi SK, Orphan VJ, Rouse GW, Jahnke L, Embaye T, Turk K *et al.* (2005). Evolutionary innovation: a bone-eating marine symbiosis. *Environ Microbiol* **7**: 1369–1378.
- Goffredi SK, Johnson SB, Vrijenhoek RC. (2007). Genetic diversity and potential function of microbial symbionts associated with newly discovered species of *Osedax* polychaete worms. *Appl Environ Microbiol* **73**: 2314–2323.
- Goodwin C, Rodolfo-Metalpa R, Picton B, Hall-Spencer JM. (2013). Effects of ocean acidification on sponge communities. *Mar Ecol* **35**: 41–49; doi:10.1111/maec.12093.
- Hall-Spencer JM, Rodolfo-Metalpa R, Martin S, Ransome E, Fine M, Turner SM *et al.* (2008). Volcanic carbon dioxide vents show ecosystem effects of ocean acidification. *Nature* **454**: 96–99.
- Hutchins DA, Fe F-X, Zhang Y, Warner ME, Feng Y, Portune K *et al.* (2007). CO₂ control of Trichodesmium N₂ fixation, photosynthesis, growth rates, and elemental ratios: implications for past, present, and future ocean biogeochemistry. *Limnol Oceanogr* **52**: 1293–1304.
- Hutchins DA, Mulholland MR, Fu F. (2009). Nutrient cycles and marine microbes in a CO₂-enriched ocean. *Oceanography* **22**: 128–145.
- IGBP, IOC, SCOR (2014). Ocean acidification summary for policymakers-third symposium on the ocean in a high-CO₂ world. International Geosphere-Biosphere Programme, Stockholm, Sweden.
- Kerfahi D, Hall-Spencer JM, Tripathi B, Milazzo M, Lee J, Adams JM. (2014). Shallow water marine sediment bacterial community shifts along a natural CO₂ gradient in the Mediterranean Sea off Vulcano, Italy. *Microb Ecol* **67**: 819–828.
- Krause E, Wichels A, Giménez L, Lunau M, Schilhabel MB, Gerdt G. (2012). Small changes in pH have direct effects on marine bacterial community composition: A microcosm approach. *PLoS One* **7**: e47035.
- Kurahashi M, Yokota A. (2007). *Endozoicomonas elysicola* gen. nov., sp. nov., a γ -proteobacterium isolated from the sea slug *Elysia ornate*. *Syst Appl Microbiol* **30**: 202–206.
- Langille MG, Zaneveld J, Caporaso JG, McDonald D, Knights D, Reyes JA *et al.* (2013). Predictive functional profiling of microbial communities using 16S rRNA marker gene sequences. *Nat Biotechnol* **31**: 814–821.
- La Rivière M, Roumagnac M, Garrabou J, Bally M. (2013). Transient shifts in bacterial communities associated with the temperate Gorgonian *Paramuricea clavata* in the Northwestern Mediterranean Sea. *PLoS One* **8**: e57385.
- Lomas MW, Hopkinson BM, Losh JL, Ryan DE, Shi DL, Xu Y *et al.* (2012). Effect of ocean acidification on cyanobacteria in the subtropical North Atlantic. *Aquat Microb Ecol* **66**: 211–222.
- Mcdonald D, Price MN, Goodrich J, Nawrocki EP, Desantis TZ, Probst A *et al.* (2012). An improved Greengenes taxonomy with explicit ranks for ecological and evolutionary analyses of bacteria and archaea. *ISME J* **6**: 610–618.
- Meakin NG, Wyman M. (2011). Rapid shifts in picoeukaryote community structure in response to ocean acidification. *ISME J* **5**: 1397–1405.
- Meron D, Atias E, Iasur Kruh L, Elifantz H, Minz D, Fine M *et al.* (2011). The impact of reduced pH on the microbial community of the coral *Acropora eurystoma*. *ISME J* **5**: 51–60.
- Meron D, Rodolfo-Metalpa R, Cunning R, Baker AC, Fine M, Banin E. (2012). Changes in coral microbial communities in response to a natural pH gradient. *ISME J* **6**: 1775–1785.
- Mohamed N, Cicerelli EM, Kan J, Chen F, Fuqua C, Hill RT. (2008). Diversity and quorum-sensing signal production of *Proteobacteria* associated with marine sponges. *Environ Microbiol* **10**: 75–86.
- Morrow KM, Moss AG, Chadwick NE, Liles MR. (2012). Bacterial associates of two Caribbean coral species reveal species-specific distribution and geographic variability. *Appl Environ Microbiol* **78**: 6438–6449.
- Moss RH, Edmonds JA, Hibbard KA, Manning MR, Rose SK, van Vuuren DP *et al.* (2010). The next generation of scenarios for climate change research and assessment. *Nature* **463**: 747–756.
- Mouchka ME, Hewson I, Harvell CD. (2010). Coral-associated bacterial assemblages: current knowledge and the potential for climate-driven impacts. *Integr Comp Biol* **50**: 662–674.
- Nishijima M, Adachi K, Katsuta A, Shizuri Y, Yamasato K. (2013). *Endozoicomonas numazuensis* sp. nov., a gammaproteobacterium isolated from marine sponges, and emended description of the genus *Endozoicomonas* Kurahashi and Yokota 2007. *Int J Syst Evol Microbiol* **63**: 709–714.
- Orr JC, Fabry VJ, Aumont O, Bopp L, Doney SC, Feely RA *et al.* (2005). Anthropogenic ocean acidification over the twentyfirst century and its impact on calcifying organisms. *Nature* **437**: 681–686.
- Padan E, Bibi E, Ito M, Krulwich TA. (2005). Alkaline pH homeostasis in bacteria: New insights. *Biochim Biophys Acta* **1717**: 67–88.
- Pike RE, Haltli B, Kerr RG. (2013). Description of *Endozoicomonas euniceicola* sp. nov. and *Endozoicomonas gorgoniicola* sp. nov., bacteria isolated from the octocorals *Eunicea fusca* and *Plexaura* sp., and an emended description of the genus *Endozoicomonas*. *Int J Syst Evol Microbiol* **63**: 4294–4302.
- Pruesse E, Quast C, Knittel K, Fuchs BM, Ludwig W, Peplies J *et al.* (2007). SILVA: a comprehensive online resource for quality checked and aligned ribosomal RNA sequence data compatible with ARB. *Nucleic Acids Res* **35**: 7188–7196.
- Raina JB, Tapiolas D, Willis B, Bourne DG. (2009). Coral-associated bacteria and their role in the biogeochemical cycling of sulfur. *Appl Environ Microbiol* **75**: 3492–3501.
- Ritchie KB. (2006). Regulation of microbial populations by coral surface mucus and mucus-associated bacteria. *Mar Ecol Prog Ser* **322**: 1–14.
- Rodriguez-Lanetty M, Granados-Cifuentes C, Barberan A, Bellantuono AJ, Bastidas C. (2013). Ecological inferences from a deep screening of the complex bacterial consortia associated with the coral, *Porites astreoides*. *Mol Ecol* **22**: 4349–4362.
- Rodriguez RJ, Henson J, Van Volkenburgh E, Hoy M, Wright L, Beckwith F *et al.* (2008). Stress tolerance in

- plants *via* habitat-adapted symbiosis. *ISME J* **2**: 404–416.
- Rua CPJ, Trindade-Silva AE, Appolinario LR, Venas TM, Garcia GD, Carvalho LS *et al.* (2014). Diversity and antimicrobial potential of culturable heterotrophic bacteria associated with the endemic marine sponge *Arenosclera brasiliensis*. *PeerJ* **2**: e419.
- Schloss PD, Gevers D, Westcott SL. (2011). Reducing the effects of PCR amplification and sequencing artifacts on 16S rRNA-based studies. *PLoS One* **6**: e27310.
- Shi D, Xu Y, Hopkinson BM, Morel FMM. (2010). Effect of ocean acidification on iron availability to marine phytoplankton. *Science* **327**: 676–679.
- Simister RL, Deines P, Botté ES, Webster NS, Taylor MW. (2012). Sponge-specific clusters revisited: a comprehensive phylogeny of sponge-associated microorganisms. *Environ Microbiol* **14**: 517–524.
- Teira E, Fernández A, Álvarez-Salgado XA, García-Martín EE, Serret P, Sobrino C. (2012). Response of two marine bacterial isolates to high CO₂ concentration. *Mar Ecol Prog Ser* **453**: 27–36.
- Todd J, Curson ARJ, Nikolaidou-Katsaraidou N, Brearley CA, Watmough NJ, Chan Y *et al.* (2012). Molecular dissection of bacterial acrylate catabolism - unexpected links with dimethylsulfoniopropionate catabolism and dimethyl sulfide production. *Environ Microbiol* **12**: 327–343.
- Uthicke S, Momigliano P, Fabricius KE. (2013). High risk of extinction of benthic foraminifera in this century due to ocean acidification. *Scientific Rep* **3**: 1769.
- Vega Thurber R, Willner-Hall D, Rodriguez-Mueller C, Desnues C, Edwards RA, Angly F *et al.* (2009). Metagenomic analysis of stressed coral holobionts. *Environ Microbiol* **11**: 2148–2163.
- Vega Thurber RL, Burkepille DE, Fuchs C, Shantz AA, McMinds R, Zaneveld JR. (2014). Chronic nutrient enrichment increases prevalence and severity of coral disease and bleaching. *Glob Change Biol* **20**: 544–554.
- Webster NS, Cobb RE, Negri AP. (2008). Temperature thresholds for bacterial symbiosis with a sponge. *ISME J* **2**: 830–842.
- Webster NS, Negri AP, Flores F, Humphrey C, Soo R, Botté ES *et al.* (2013a). Near-future ocean acidification causes differences in microbial associations within diverse coral reef taxa. *Environ Microbiol Rep* **5**: 243–251.
- Webster NS, Uthicke S, Botté ES, Flores F, Negri AP. (2013b). Ocean acidification reduces induction of coral settlement by crustose coralline algae. *Glob Change Biol* **19**: 303–315.
- Wilkinson CR. (1983). Net primary productivity in coral reef sponges. *Science* **219**: 410–412.
- Witt V, Wild C, Anthony KRN, Diaz-Pulido G, Uthicke S. (2011). Effects of ocean acidification on microbial community composition of, and oxygen fluxes through, biofilms from the Great Barrier Reef. *Environ Microbiol* **13**: 2976–2989.
- Yang CS, Chen MH, Arun AB, Chen CA, Wang JT, Chen WM. (2010). *Endozoicomonas montiporae* sp. nov., isolated from the encrusting pore coral *Montipora aequituberculata*. *Int J Syst Evol Micr* **60**: 1158–1162.
- Zaneveld JR, Vega Thurber RL. (2014). Hidden State Prediction: a modification of classic ancestral state reconstruction algorithms helps unravel complex symbioses. *Front Microbiol* **5**: 431.



This work is licensed under a Creative Commons Attribution-NonCommercial-ShareAlike 3.0 Unported License. The images or other third party material in this article are included in the article's Creative Commons license, unless indicated otherwise in the credit line; if the material is not included under the Creative Commons license, users will need to obtain permission from the license holder to reproduce the material. To view a copy of this license, visit <http://creativecommons.org/licenses/by-nc-sa/3.0/>

Supplementary Information accompanies this paper on The ISME Journal website (<http://www.nature.com/ismej>)